Ignition Delay Correlation for Engine Operating with Lean and with Rich Fuel-Air Mixtures

Author, co-author (Do NOT enter this information. It will be pulled from participant tab in MyTechZone)

Affiliation (Do NOT enter this information. It will be pulled from participant tab in MyTechZone)

Abstract

An ignition delay correlation encompassing the effects of temperature, pressure, residual gas, EGR, and lambda (on both the rich and lean sides) has been developed. The procedure uses the individual knocking cycle data from a boosted direct injection SI engine (GM LNF) operating at 1250 to 2000 rpm, 8-14 bar GIMEP, EGR of 0 to 12.5%, and lambda of 0.8 to 1.3 with a certification fuel (Haltermann 437, with RON=96.6 and MON=88.5). An algorithm has been devised to identify the knock point on individual pressure traces so that the large data set (of some thirty three thousand cycles) could be processed automatically. For lean and for rich operations, the role of the excess fuel, air, and recycled gas (which has excess air in the lean case, and hydrogen and carbon monoxide in the rich case) may be treated effectively as diluents in the ignition delay expression.

Introduction

Boosted down-size engine is a successful strategy for improving fuel economy [1, 2]. Because of the reduced displacement, the engine operates at high mean effective pressure which renders it prone to knock. Therefore, it is of importance to be able to assess the engine knock tendency through modelling. The modelling usually takes two steps [3]. Firstly, the ignition delay of the fuel air mixture is determined as a function of pressure and temperature. Then, using the Livengood- Wu integral method [4], this delay is connected to the pressure-temperature trajectory in the engine end gas to see whether the end gas chemistry has progressed to the knock point in the engine cycle.

Three are three approaches to determine the expression of ignition delay of fuel-air mixtures as a function of temperature and pressure:

(i)   Experimental determination through measurements in a rapid compression machine [5] or a shock tube [6]
(ii) Kinetic modeling of the pre-ignition chemistry of the fuels [7] or their surrogates [8, 9]
(iii) Correlations of ignition delay data from engines [10, 11]

The subject of this paper belongs to category (iii) of the above. The correlation of Douaud and Eyzat [10], which is widely used, has been extended to modern turbo-charged engine with EGR by Hoepke et al [11]. The correlation is further extended here to encompass fuel lean and fuel rich mixtures. It should be noted that the current work is based on one fuel (a calibration gasoline similar to the premium gasoline sold in US), and therefore, does not address the fuel effects on ignition delay. The effects of octane number and alcohol blending will be addressed in future work.

Methodology

The approach is to obtain an ignition delay correlation based on the individual cycle pressure data for a modern turbo-charged engine operating over a wide range of operating conditions. Because of the engine cycle-to-cycle variations, there is a substantial set of realization even at the same operating point.

Engine and operating conditions

The data were collected using a production 2L turbo-charge engine (GM LNF engine). The engine specifications are shown in Table 1. An experimental engine ECU provided by GM was employed so that the valve timing, fuel injection timing, and turbo-waste gate position were controlled with the factory calibration. The value for λ and spark timing were specified by the user. A low pressure EGR loop had been added to the engine which was originally not equipped with EGR provision. The exhaust was not throttled to avoid disruption of the turbine operation; as a result, the maximum EGR level was limited to 12.5%.

Table 1. Engine specification; the valve timings are functions of speed and load. The tabulated values are for 1500 rpm and 14 bar GIMEP for reference.

Engine type	Turbocharged in-line 4
Displaced volume	2L
Bore/ Stroke	86mm/ 86 mm
Compression ratio	9.2
IVO (@1500 rpm, 14 bar GIMEP)	31° btdc gas exchange
IVC (@1500 rpm, 14 bar GIMEP)	19° abdc compression
EVO (@1500 rpm, 14 bar GIMEP)	18° bbdc expansion
EVC (@1500 rpm, 14 bar GIMEP)	22 atdc gas exchange

To obtain a large data set that would cover many parameters for the correlation, the engine was operated over an extensive range of conditions; see Table 2. The load range of 8-14 bar encompassed both turbo- and non-turbo- operations. The spark timing was swept to obtain light to heavy knock. Altogether there were 336 operating

7/20/2015

points, and 99 consecutive cycles; thus there were 336x99 = 33264 data points for the correlation. The pressure data were acquired at 100 KHz.

Speed	1250 – 2000 rpm
GIMEP	8 – 14 bar
Spark timing	Various; from light to heavy knock
λ	0.8 to 1.3
EGR	0 to 12.5%

Determining the knock point

It is necessary to identify the "knock point" in the individual pressure trace for the correlation development. Because of end gas non-uniformity (in both temperature and composition), auto-ignition occurs locally at exothermic centers [12]. The pressure sensor responds to the pressure wave generated by the local heat release. Because of the unknown relative location of the exothermic center and the pressure transducer, there is an inherent delay in detecting the "knock point", which may be defined as the time of the start of the rapid auto-ignition heat release, from the pressure trace. The worst case scenario is that the exothermic center is diametrically opposite to the sensor. For the engine under test, the corresponding pressure wave travel time is of the order of 100 μs. The actual delay should be less than that.

A pressure (p) trace showing the knock phenomenon, and the high frequency component ($\hat{p}$) are shown in Fig. 1 (a) and (b) respectively. The latter has been obtained by filtering the pressure signal via a phase-conserving high-pass filter [13] with a cut-off frequency at 2.5 KHz. The result is not sensitive to the cut-off frequency as long as it can discriminate against the normal cycle pressure variation. In Fig. 1(a), the pressure starts to rise rapidly at 20.87 ms from BDC. (For this case, engine ran at 1500 rpm; 21 ms from BDC corresponds to 9° crank angle ATDC.) This point is marked as the blue circle in Fig. 1(a) and it may be considered as the knock (or auto-ignition) point on the pressure trace. The knock on-set threshold has been set at $|\hat{p}| = 1$ bar. The point where $\hat{p}$ crosses the threshold is marked as the yellow square in Fig. 1. There is a substantial difference in time for the points marked by the blue circle and by the yellow square. Thus a knock point determined by setting a discrimination level on $\hat{p}$ may overestimate the ignition delay.

Although identifying the knock point on the pressure trace is easy by eye, an algorithm has to be established for processing the large set of pressure data (more than thirty thousand for this study). The algorithm used is based on the integral of the modulus of pressure oscillation (IMPO):

$$i_o(t) = \int_{t_0}^{t} |\hat{p}(t')| dt' \qquad (1)$$

where t_0 is sometime before the knock event (the precise definition is immaterial, as only changes in i_0 are sought), and t is the running time. When evaluated for a fixed interval of time (i.e., for a specified t), i_0 has been used as a scaler knock metric [14]. The value i_0 is akin

to the cumulative acoustic energy of the pressure wave passing through the pressure transducer (in that case, $\hat{p}^2$ instead of $|\hat{p}|$ would be used as the integrand).
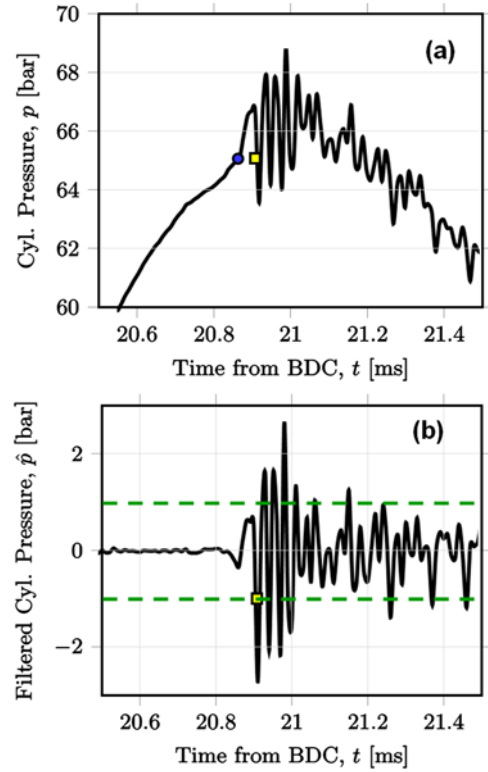

Figure 1. (a) Pressure trace showing the knock phenomenon. (b) High frequency component above 2.5KHz. Dash lines mark the knock threshold amplitude of 1 bar. Data at 1500 rpm; 21 ms from BDC corresponds to 9° ATDC-compression.
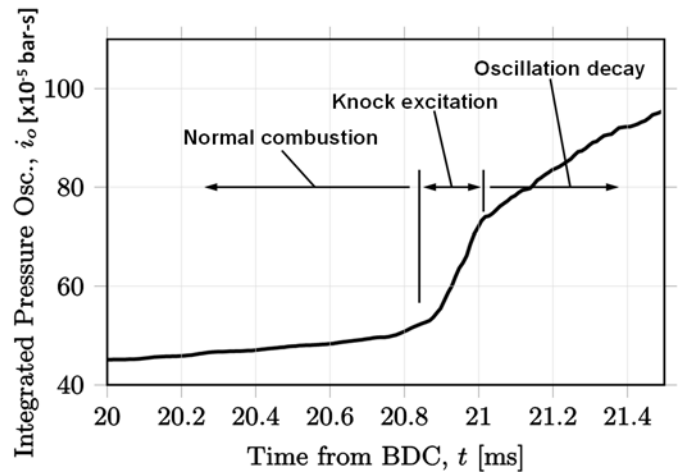

Figure 2. .Integral of the modulus of pressure oscillation, $i_0(t)$, for the pressure oscillation shown in Fig. 1 (b).

The value of $i_0(t)$ is shown in Fig. 2 for the pressure oscillation shown in Fig. 1(b). Three regimes are identified. On the left of the figure, the slow increase in i_0 is due to the accumulation of the absolute value of the pressure noise in normal combustion. (If there were no noise, the trace would have been flat.) Then there is the rapid rise due to the arrival of the pressure wave. Finally, the pressure oscillation decay as the piston descents.

The start of the knock excitation region may be taken as the knock point. This point may be determined by the intersection of the line representing the rise of i_0 due to normal combustion, and the line representing that due to the presence of the pressure wave. Procedure wise, a window of data starting from 250 μs before the appearance of any oscillation to 100 μs after the peak $\hat{p}$ point is selected. Then two straight line segments intersecting at the knock point are constructed. (The four parameters, two slopes and two intercepts of the lines, completely determine the lines and the intersection.) The knock point is selected by choosing the four parameters to minimize the square of the difference between the line segments and the data in the window. In practice, this window may sometimes extend beyond the knock excitation region and create fit error; see Fig. 3. The resulting knock point, however, is not materially affected. For this case, the determined knock point at 20.87 ms from BDC is the same as the value determined by eye in Fig. 1(a).
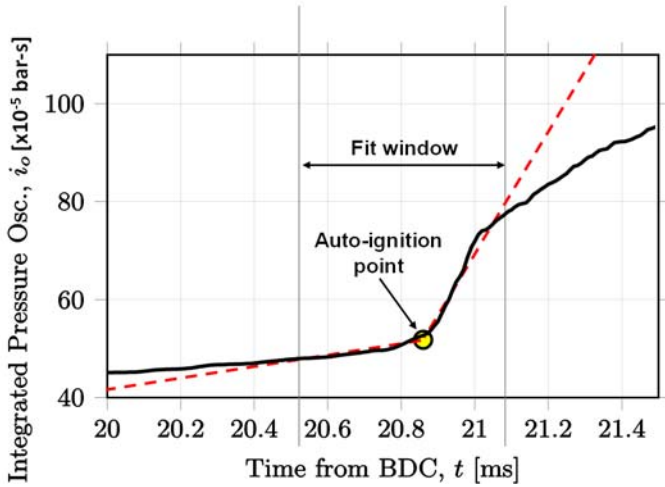

Figure 3. Fitting of line segments in the fit window to determine the knock point for data in Fig. 1 and 2. Although the window used extends beyond the knock excitation region resulting in some errors in the line fit, the knock point location is not materially affected.

Cycle p-T trajectory

The ignition delay correlation was developed by fitting an expression τ(p,T) to the p-T trajectory leading to knock in the individual cycle data. The instantaneous pressure in the cycle was measured. The corresponding temperature was calculated from the isentropic compression of the end gas using real gas properties. The initial temperature used in this calculation was the charge temperature at IVC obtained by a cycle simulation program [15] using the mean values of the engine parameters at the operating point. Thus although there was a cycle-to-cycle variation in the p-T trajectory in every cycle at the same operating point, the initial temperature (at IVC) was the same.

Fitting the Ignition Delay to Data

The selected functional form of the ignition delay expression is:

$$\tau\left(p,t;\lambda,EGR\right)=a\left(\frac{p}{T}\right)^{-b} e^{\frac{c}{T}} f\left(\lambda,EGR\right) \qquad (2)$$

Instead of using a p dependence, the (p/T) term in the pre-exponential reflects the density dependence of τ [11], since kinetic rates are

directly dependent on concentrations rather than pressure. The factor f accounts for a separable λ - EGR dependence from the p -T dependence.

The fit of the τ expression to data is as follows. For every knocking cycle, an auto-ignition time $\hat{t}_{ign}$ may be computed from the Livengood - Wu integral based on Eq.(1) and p-T trajectory of that cycle if the coefficients a, b, c and the function f are known:

$$1=\int_{t_{IVC}}^{\hat{t}_{ign}} \frac{dt'}{\tau(p(t'),T(t');\lambda,EGR)} \qquad (3)$$

The $\hat{t}_{ign}$ is compared to the observed knock point time (t_{ign}) of the cycle, and the coefficients a, b, c, and function f are chosen to minimize the mean square error E

$$E=\frac{1}{N}\sum_{i=1}^{N}\left(\hat{t}_{ign}-t_{ign}\right)_i^2 \qquad (4)$$

The sum is over all the operating points and individual cycles at each operating point.

Fit to Stoichiometric Data

The data fit was first applied to the run matrix with λ = 1. The sub-data set is listed in Table 3.

Table 3. Matrix of operating points for λ = 1 data set

Speed (rpm)	GIMEP (bar)	Spark (° atdc)	EGR (%)	λ
1250	8 to 9	-25 to -35	0 to 8	1
1500	10 to 14	-10 to -42	0 to 12.5	1
1750	10 το 14	-18 to -45	0 το 12.5	1
2000	11 to 14	-22 to -42	0 to 12.5	1

At λ = 1, the recycled exhaust gas serves as a diluent. However, at the lower load, the residual gas fraction also needs to be accounted for. Therefore a diluent fraction w_d is defined by the sum of the two:

$$w_d = EGR + x_r \qquad (5)$$

The definitions of EGR and residual gas fraction x_r are listed at the end of the paper. The residual gas fraction was obtained by engine simulation at the mean engine condition at the operation point [15]. Then the factor f in Eq. (2) is modeled as a power law dependence on (1-w_d):

$$f(\lambda=1)=\left(1-w_d\right)^{-d} \qquad (6)$$

The expression for the fit at λ = 1 is

$$\tau(ms)=2.71x10^{-5}\left(\frac{p(bar)}{T(K)}\right)^{-1.73} e^{\frac{5190}{T(K)}}\left(1-w_d\right)^{-0.618} \qquad (7)$$

The comparison between the observed knock point and the one calculated using Eq.(7) and Eq.(3) are shown in Fig.4, which shows very good agreement between the observed and calculated values.
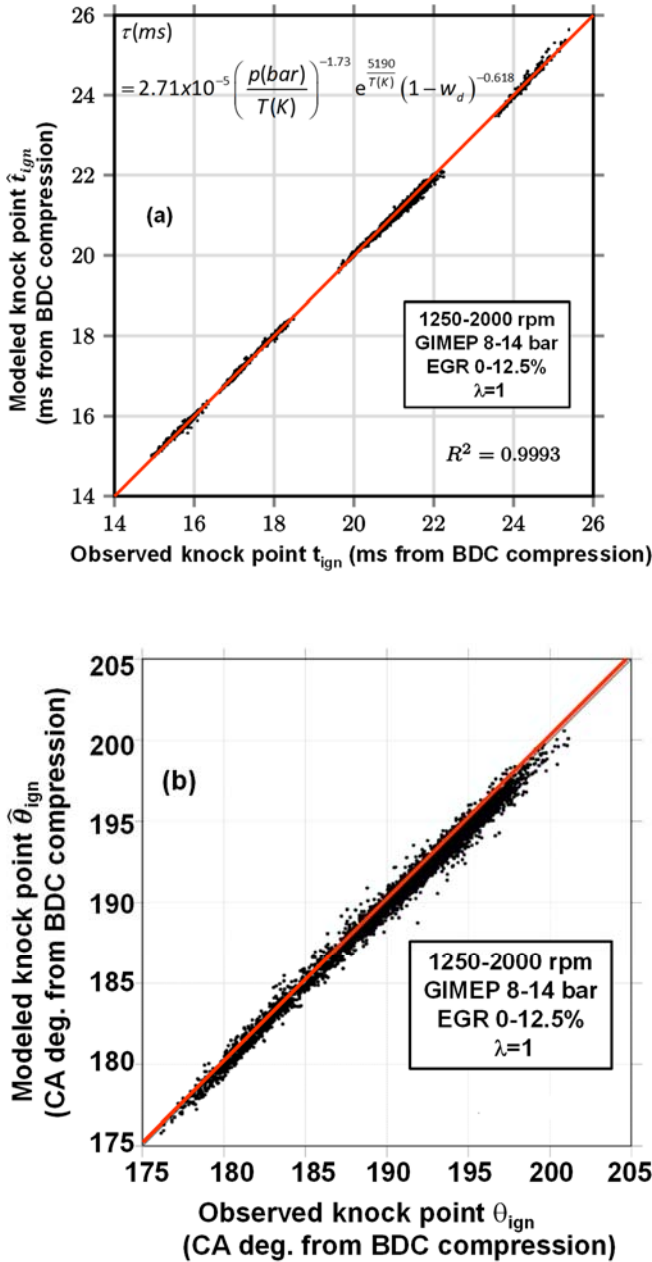

Figure 4. Comparing modeled and observed knock points at $\lambda = 1$.
(a) Comparing in terms of time of auto-ignition; (b) comparing in terms of crank angle of ignition. The 45° line represents perfect fit.

Fit to $\lambda \neq 1$ data

Table 4 shows the test matrix for non-stoichiometric ignition delay data set. When the charge is lean or rich, to the lowest order of approximation, the mixture is diluted by the excess air or by the excess fuel, although the stoichiometry may affect the pre-ignition chemistry. So the correlation strategy is to treat the excess air or excess fuel simply as a diluent first. Further modification for the

ignition delay as a function of λ due to chemistry effects may be made if necessary.

Table 4. Matrix of operating points for $\lambda \neq 1$ data set

Speed (rpm)	GIMEP (bar)	Spark (° atdc)	EGR (%)	λ
1250	8 to 9	-25 to -35	0 to 8	0.8-1.3; $\lambda \neq 1$
1500	10 to 14	-10 to -42	0 to 12.5	0.8-1.3; $\lambda \neq 1$
1750	10 to 14	−18 to −45	0 to 12.5	0.8-1.3; $\lambda \neq 1$
2000	11 to 14	-22 ot -42	0 to 12.5	0.8-1.3; $\lambda \neq 1$

Fuel lean ($\lambda > 1$)

The excess air mass fraction is given by

$$\delta = \frac{m_a - m_{a,stoi}}{m_a + m_f} = \frac{\lambda - 1}{\lambda + (F/A)_{stoi}} \quad (8)$$

For lean mixture, $\delta > 1$. The dilution fraction of Eq. (5) is modified as:

$$w_d = EGR + x_r + k_L \delta \quad (9)$$

The factor K_L has been introduced to account for the difference between the dilution effect of excess air and burned gas. Then Eq. (7) is fit to the fuel lean data by adjusting K_L only, with all the other coefficients unchanged from the stoichiometric fit.

Fuel rich ($\lambda < 1$)

The air deficit fraction is given by the same expression as in Eq. (8), but now the value of δ is negative. The excess fuel mass fraction is:

$$\frac{m_f - m_{f,stoi}}{m_a + m_f} = (-\delta)(F/A)_{stoi} \quad (10)$$

The dilution fraction of Eq.(5) is modified as:

$$w_d = EGR + x_r + k_R \left[(-\delta)(F/A)_{stoi} \right] \quad (11)$$

The factor K_R has been introduced to account for the difference between the dilution effect of excess fuel and burned gas. Then Eq. (7) is fit to the fuel rich data by adjusting K_R only, with all the other coefficients unchanged from the stoichiometric fit.

Overall fit

Fit to the fuel lean and fuel rich cases respectively showed that very good results were obtained with the values of K_L and K_R given by:

$$K_L = K_R (F/A)_{stoi} = 0.95 \quad (12)$$

Since the dilution factor only addresses the physical effects, the result that K_L is slightly less than 1 may be attributed to the fact that the specific heat of air is less than that of the burned gas. That K_R is an order of magnitude large than K_L (since $(F/A)_{stoi} = 1/14.6$) may be

attributed to the fact that the specific heat of fuel vapor is much larger (approximately by an order of magnitude) than that of air.

Comparisons between the modeled and observed knock point for the non-stoichiometric data set are shown in Fig. 5. With the good agreement between the model and the data, further refinement of the correlation to account for the stoichiometric effect beyond dilution is deemed not necessary.
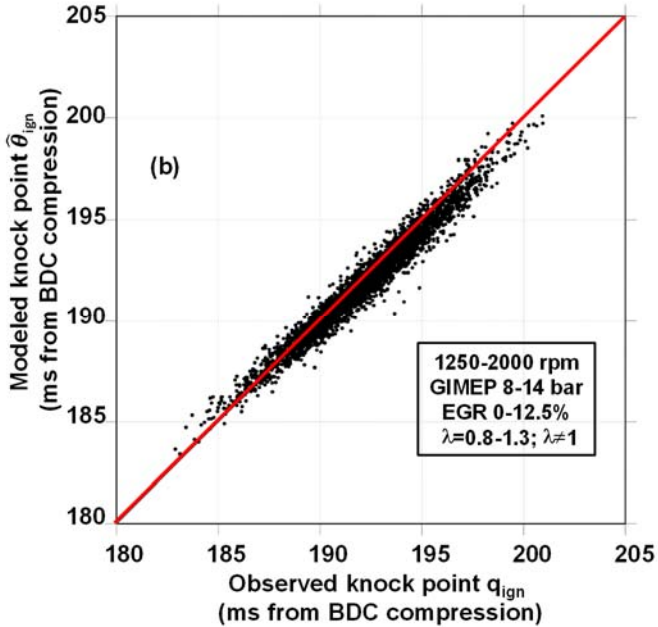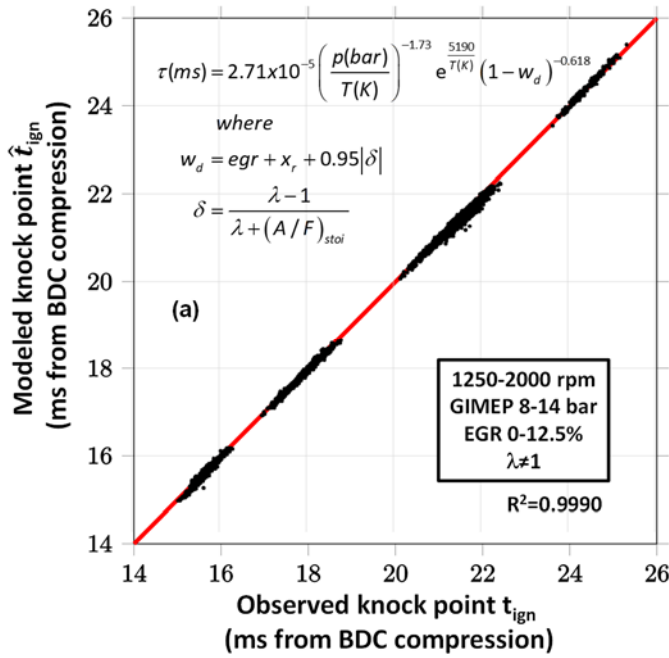

Figure 5. Comparing modeled and observed knock points for $\lambda \neq 1$. (a) Comparing in terms of time of auto-ignition; (b) comparing in terms of crank angle of ignition. The 45° line represents perfect fit.

Summary/Conclusions

An ignition delay correlation has been developed to include the effect of EGR and λ. The data set encompasses speed of 1250 to 2000 rpm, EGR of 0 to 12.5%, and λ of 0.8 to 1.3. The effects of EGR and departure of mixture from stoichiometric are taken as dilution effects. The ignition delay correlation is

$$\tau(ms) = 2.71 \times 10^{-5} \left(\frac{p(bar)}{T(K)} \right)^{-1.73} e^{\frac{5190}{T(K)}} \left(1 - w_d \right)^{-0.618}$$

where

$$w_d = egr + x_r + 0.95|\delta|$$

$$\delta = \frac{\lambda - 1}{\lambda + (A/F)_{stoi}}$$

(13)

There is good agreement between the knock point (auto-ignition time) calculated by the correlation and observation.

References

1. Lake, T., Stokes, J., Murphy, R. Osborne, R., Schamel, A., "Turbocharging Concepts for Downsized DI Gasoline Engines," SAE 2004-01-0036, 2004.
2. Petitjean, D., Bernardini, L., Middlemass, C., Shahed, S.M., "Advanced Gasoline Engine Turbocharging Technology for Fuel Economy Improvements," SAE 2004-01-0988, 2004.
3. Heywood, J, *Internal Combustion Engine Fundamentals*, McGraw –Hill, ISBN 0-07-028637, 1988.
4. Livengood, J.C., Wu, P.C., "Correlation of Autoignition Phenomena in Internal Combustion Engines and Rapid Compression Machines," *5th Symp. (Int.) on Combustion*, 347-356, Reinhold Publ. Corp., 1955.
5. Minetti, R. Carlier, M., Ribaucour, M., Therssen, E., and Sochet, L.R., "A Rapid Compression Machine Investigation of Oxidation and Auto-Ignition of n-Heptane: Measurements and Modeling*," Comb. & Flame*, 102, 298-309, 1995.
6. Fieweger, K., Blumenthal, R., and Adomeit, G., "Self-Ignition of SI Engine Model Fuels: A Shock Tube Investigation at High Pressure," *Comb. & Flame*, 109, pp599-619, 1997.
7. Cox, R.A., Cole, J.A., "Chemical Aspects of the Autoignition of Hydrocarbon-Air Mixtures," *Comb. & Flame*, 60, 109-123, 1985.
8. Westbrook, C.K., Warnatz, J., and Pitz, W.J., "A Detailed Chemical Kinetic Reaction Mechanism for the Oxidation of iso-Octane and n-Heptane over an Extended Temperature Range and its Applications to Analysis of Engine Knock," *22nd Symp. (Int.) on Combustion*, 893, The Combustion Institute, 1988.
9. Kalghatgi, G., Babiker, H., and Badra, J., "A Simple Method to Predict Knock Using Toluene, N-Heptane and Iso-Octane Blends (TPRF) as Gasoline Surrogates," SAE Paper 2015-01-0757
10. Douaud, A., Eyzat, P., "Four-Octane-Number Method for Predicting the Anti-Knock Behavior of Fuels and Engines," SAE Paper 780080, 1980.
11. Hoepke, B., Jannsen, S., Kasseris, E., and Cheng, W.K., "EGR Effects on Boosted SI Engine Operation and Knock Integral Correlation," SAE Paper 2012-01-0707, 2012.
12. Konig, G, Maly, R.R., Bradley, D., Lau, A.K.C., and Sheppard, C.G.W., "Role of Exothermic Centres on Knock Initiation and Knock Damage," SAE Paper 902136, 1990.

13. The "filtfilt" function in *Matlab Signal Processing Toolbox*, The Math Works Inc.
14. Cavina, N., Corti, E., Minelli, G., Moro, D., and Solieri, L., "Knock Indexes Normalization methodologies," SAE Paper 2006-01-2998, 2006.
15. *GT-Power*, Gama Technology.

Contact Information

Contact details for the main author should be included here. Details may include mailing address, email address, and/or telephone number (whichever is deemed appropriate).

Acknowledgments

Definitions/Abbreviations

$(A/F)_{stoi}$	Stoichiometric Air Fuel ratio
ATDC	After-top-dead-center
BDC	Bottom-dead-center
EGR	Exhaust gas recirculation $= m_{EGR}/(m_a+m_f)$
EVO/ EVC	Exhaust valve open/ close
GIMEP	Gross indicated mean effective pressure
IVO/ IVC	Intake valve open/.close
i_0	Integral of modulus of pressure oscillation; see Eq. (1)
m_a	Air mass
m_{egr}	EGR mass
m_f	Fuel mass
m_r	Residual mass
p	Pressure
$\hat{p}$	Pressure oscillation
T	Time
t_{ign}	Time at auto-ignition (knock point)
$\hat{t}_{ign}$	Computed time at auto-ignition (knock point)
T	Temperature
w_d	Dilution fraction
x_r	Residual gas fraction; $=m_r/(m_a+m_f)$
δ	Excess air mass fraction; See Eq. (8)
λ	Air equivalence ratio
τ	Ignition delay